EFFECTS OF NOZZLE DESIGN AND POWER ON CRUISE DRAG FOR UPPER-SURFACE-BLOWING AIRCRAFT

Edward T. Meleason
NASA Lewis Research Center

SUMMARY

A high-speed wind-tunnel investigation was conducted on a series of upper-surface-blowing nozzles with D-shaped exits installed on a representative short-haul aircraft model. Both two- and four-engine configurations were investigated. Powered engine simulators were used to properly represent nacelle flows. Large differences in cruise drag penalties associated with the various nozzle designs were seen. Some geometric parameters influencing nozzle cruise drag are identified.

INTRODUCTION

Upper-surface-blowing (USB) nozzle design requirements present a conflict between good low-speed and high-speed performance, as noted in reference 1. At low speeds, a relatively wide, thin jet is desired for good flow turning and lift augmentation (ref. 2). This is usually accomplished by directing the nozzle jet onto the wing upper surface with a high boattail angle nozzle. Conversely, low boattail angles and minimal jet spreading appear desirable for low cruise drag. Previous investigators have reported (ref. 3) that compromising all the nozzle design parameters toward favorable low speed flow turning increased the cruise drag by as much as 20 percent of the airplane drag.

This earlier work involved the development of a USB nozzle for a configuration with twin high-pressure-ratio (low bypass ratio) engines. The present investigation was directed toward cruise nozzles for low-pressure-ratio USB engines similar to those being developed under NASA's QCSEE (Quiet, Clean, Short-Haul Experimental Engine) Program (ref. 4). A later paper by Ciepluch summarizes features of the QCSEE propulsion system. The different cruise nozzle exit geometries required for the different pressure ratio engines are shown in figure 1. The QCSEE nozzle exit is larger relative to its nacelle, producing a lower aspect ratio nozzle with sharper corners. In the present test, all experimental nozzles had this D-shaped low-aspect-ratio nozzle exit geometry. Cruise drag was evaluated for both low boattail angle nozzles designed specifically for good cruise drag and also for high boattail angle nozzles representing the QCSEE USB design. Both two- and four-engine configurations were tested.

SYMBOLS

A_{BT}	boattail projected area above the wing, cm^2 (in^2)
A_{EXIT}	nozzle exit area, cm^2
A_{NAC}	maximum circular cross-sectional area of nacelle, cm^2 (in^2)
AR_{EXIT}	exit aspect ratio, width/height
C_D	drag coefficient, $drag/q_0S$
C_L	lift coefficient, $lift/q_0S$
C_P	pressure coefficient, $(p-p_0)/q_0S$
M_0	free-stream Mach number
p_0	free-stream static pressure, N/cm^2
q_0	free-stream dynamic pressure, N/cm^2
S	wing area, cm^2 (in^2)
W	width, cm (in.)
β_{TOP}	external top centerline boattail angle at nozzle exit, deg
β_{SIDE}	external sidewall boattail angle at nozzle exit, deg
Δh	maximum displacement of external boattail corner, cm (in.)
θ_{KD}	average of top and bottom centerline flow deflection angles at nozzle exit

MODEL DESCRIPTION

Figure 2 is a photograph of the half-plane model installed in the Lewis Research Center's 8- by 6-Foot Supersonic Wind Tunnel. The 0.7-m (27.5-in.) semispan model was designed for Mach 0.7 cruise and had a cylindrical fuselage and straight supercritical wing. Wing sweep at the quarter chord was 5.6° and the aspect ratio was 7.0. The wing had a taper ratio of 0.3 and an average section thickness of about 13.5 percent. The entire aerodynamic configuration was mounted on a 6-component balance. Powered engine simulators, nominally 7.6 cm (3 in.) in diameter, were used to represent the nacelle flows. Flow-through nacelles were also used.

A typical nozzle installation on the wing is shown in figure 3. Inboard

nacelle centerline position was at 23 percent of semispan, with the outboard nacelle at 48 percent. The nozzle exits were located at 35 percent of the local chord, and the exit plane was unswept in the lateral direction.

The experimental nozzle designs are shown in figure 4. All had D-shaped exits with an aspect ratio (width/height) of about 2. The reference nozzle, designated N_{REF}, had a moderate external top (crown line) boattail angle of about 11° and an external side boattail of about 2°. The QCSEE-type nozzles, N_{QC}, featured a high external top boattail angle of 28° in order to obtain a high kickdown angle and to avoid internal flow restrictions at the larger exit area required at takeoff. Because of the high kickdown angle (average centerline kickdown angle, $\theta_{KD} = 12°$), this type of nozzle would not require some type of flow deflector for good low-speed powered-lift performance as low-angle nozzles like N_{REF} would. The sidewall boattailing of the QCSEE N_{QC} nozzles (17° external, 10° internal) was designed to minimize jet spanwise pluming at cruise. Note that because N_{REF} is mounted lower on the wing than N_{QC} the boattail projected area above the wing is reduced.

There are two versions of the QCSEE nozzle, designated BL (baseline) and RC1 (recontoured no. 1). As discussed in an earlier paper by Sleeman and Phelps, the original baseline QCSEE nozzle was recently changed to the RC1 contour to improve its low-speed powered-lift characteristics. Note that the effect of the change was to flatten the top of the nozzle, increase the sharpness of the corners, and increase the effective boattail angle particularly at the corners. The terminal boattail angles on the top, β_{TOP}, and side, β_{SIDE}, remained unchanged. On the model, the external nozzle contours for $(N_{QC})_{BL}$ and $(N_{QC})_{RC1}$ correspond to the baseline and recontoured QCSEE configurations; however, the internal contours for both were for the baseline nozzle. In addition to these configurations, some modified versions of the N_{QC} nozzles were also tested.

The model N_{QC} nozzles were not an exact scaled representation of the full-scale QCSEE nozzle installation. During model design it became necessary to increase the nacelle maximum diameter to provide more room for instrumentation routing. As shown in figure 5, this added additional area to the forward part of the nozzle boattail and reduced the local curvature slightly. The high angle part of the boattail near the nozzle exit was duplicated exactly. The influence of this boattail area difference on the experimental results is addressed later in this paper.

POWERED SIMULATOR CONSIDERATIONS

Calibration

Prior to the wind-tunnel test, the propulsion nacelles with engine simulators were calibrated statically. A plate simulating the wing upper surface contour was attached to the nozzle through a separate balance, and its drag contribution was deleted. Nozzle thrust in the axial direction was calibrated as a function of nozzle pressure ratio for each experimental simulator/nozzle combination.

Drag Definition

Cruise drag results are presented in terms of a drag penalty which is described in figure 6. The drag penalty is the difference between the drag of the combined nacelle/wing-body configuration minus the separate isolated drags of the nacelle and wing-body. The total configuration drag with power consisted of the balance drag force corrected for the net thrust of the powered nacelles. The external nacelle drag was estimated for an assumed isolated nacelle at free-stream Mach number using an empirical technique based on nacelle fineness ratio. This estimate did not account for the increased pressure drag that would be present on an isolated high boattail nozzle such as the QCSEE nozzle. The drag of the basic wing-body without nacelles was measured. This drag was evaluated at values of Mach number and lift coefficient identical to those of the nacelle-on configuration. An additional correction was made to account for the drag increment of that portion of the wing covered by the nacelle. With these various drag components deducted from the original configuration drag, the remaining increment was considered a drag penalty which included any unfavorable interference effects. It should be noted that the scrubbing drag of the jet flow on the wing upper surface was not accounted for and would be included as part of the drag penalty.

Power Effects

Figure 7 is a typical comparison of drag results obtained with the powered simulators and with flow-through nacelles at Mach 0.7. The design point indicates the design lift coefficient of the model wing and the cruise fan pressure ratio of the QCSEE engine. For reference, a drag increment equivalent to 5 percent of cruise net thrust (airplane drag) is indicated, and it is seen that the power effect can exceed this value. Note that at the higher lift coefficient the jet flow has a favorable effect on drag. However, this favorable effect is small compared to the higher drag levels seen at this C_L.

RESULTS AND DISCUSSION

Two-Engine Configurations

Experimental drag penalties for the N_{REF} and $(N_{QC})_{BL}$ nozzle installations are shown in figure 8 for a two-engine airplane configuration (single nacelle installed on the half-plane wind-tunnel model). The powered nacelle was located at the inboard position (23 percent semispan), and data are shown for a fan pressure ratio of 1.37 and a lift coefficient of 0.4, corresponding to Mach 0.7 cruise design conditions. At these conditions, the nozzle pressure ratio was about 1.9 based on free-stream static pressure and about 2.2 based on local static pressure. At the design Mach number of 0.70, the reference nozzle N_{REF} had a small drag penalty of about 1.5 percent of net thrust (or airplane drag). Most of this penalty was probably associated with the additional scrubbing drag

of the jet on the wing. The high boattail angle baseline QCSEE nozzle $(N_{QC})_{BL}$ exhibited a considerably higher drag penalty at Mach 0.7, amounting to about 5 percent of net thrust. This penalty was partly associated with lower pressures over the nozzle boattail, as will be seen later. In addition, an enlarged region of supercritical flow was present on the wing upper surface with this nozzle. The wing shock was strengthened and moved aft toward the nozzle exit from its clean wing position.

Note that as Mach number increased beyond design, the reference nozzle developed a favorable interference effect while the drag of the N_{QC} nozzle continued to increase. Wing pressure data indicate that the reference nozzle acted to retard the development of supercritical flow above the wing as the wing entered drag rise, while the higher angle N_{QC} nozzle did not.

Four-Engine Configurations

Cruise drag results are presented in figure 9 for the four-engine configuration with reference nozzles N_{REF}, baseline QCSEE nozzles $(N_{QC})_{BL}$, and recontoured QCSEE nozzles $(N_{QC})_{RC1}$. A large difference in drag levels is evident. At Mach 0.70, the reference nozzles again had a relatively low drag penalty of less than 3 percent of net thrust. This is slightly less than twice the two-engine value for this nozzle, indicating the absence of any unfavorable nacelle-to-nacelle interference effects. The drag penalty with the N_{QC} baseline nozzles was about 12 percent of net thrust at Mach 0.7; twice the twin-engine value would be about 9 percent. Therefore, an additional drag penalty of about 3 percent is indicated due to nacelle-to-nacelle interference for this design. These mutual interference effects are also evident from the wing pressure data. With the N_{QC} nozzles, the addition of the outboard nacelle resulted in an accelerated supercritical flow region in the channel between the nozzles.

The change in external contour shape from the $(N_{QC})_{BL}$ configuration to the $(N_{QC})_{RC1}$ configuration produced an additional large drag increase (from 12 to 18 percent of net thrust at Mach 0.7). This was associated with extensive flow separation over the aft part of the $(N_{QC})_{RC1}$ boattail, as shown in figure 10. The crown line pressure distributions for the three nozzles are considerably different. A region of supercritical flow existed on the $(N_{QC})_{RC1}$ boattail, and extensive separation was present on the aft boattail, as indicated by the reduced pressure recovery at the trailing edge and shown on the tuft photograph. Flow over the $(N_{QC})_{BL}$ boattail approached the sonic level and only a small separation region was present. The N_{REF} boattail flow was at a nearly constant subsonic level.

Four-Engine Configurations with Modified Nozzles

The relatively high drag levels observed with the N_{QC} nozzles led to the development of modified N_{QC} nozzle configurations to further investigate drag behavior. These modified nozzles, shown in figure 11, were fabricated by add-

ing material externally to the boattail region of the N_{REF} nozzles. The external crown lines of the baseline and RC1 configurations were duplicated from the nozzle exit forward until fairing was required to match the maximum height of N_{REF}. As mentioned earlier, since N_{REF} was mounted lower on the wing than N_{QC}, a reduced boattail projected area above the wing resulted. Cross-sectional contours were similarly duplicated and shifted to match the very shallow sidewall boattail angles of N_{REF}. The resulting configurations thus had external boattail tops and corners quite similar to the N_{QC} nozzles, but with reductions in sidewall boattailing, boattail projected area, and flow kickdown angle on the wing. The modified nozzles are designated as $MOD(N_{QC})_{BL}$ and $MOD(N_{QC})_{RC1}$.

The combination of these changes produced a significant reduction in cruise drag at all Mach numbers. As shown in figure 12, a similar reduction occurs with the modified nozzles for both the RC1 and baseline boattails. In both cases the modifications alleviated the region of supercritical flow on the wing upper surface near the nozzles. Although not determined specifically, it appears probable that the mutual interference between nacelles was reduced with the modified configurations. It is seen from figure 12 that the external boattail change from baseline (BL) to the recontoured shape (RC1) produced similar large drag increases for both the unmodified and modified nozzles. Extensive boattail flow separation similar to that seen previously with $(N_{QC})_{RC1}$ was again observed on the $MOD(N_{QC})_{RC1}$ configuration.

Geometric Effects

The difference in external boattail geometry between baseline and recontoured configurations is predominantly an increased sharpness of the local nozzle corners. In figure 13 drag is correlated against a corner sharpness parameter $\Delta h/(W/2)$, where Δh is the maximum corner displacement from a line connecting the intersections of the nacelle centerlines with the nozzle crown line and side, and $W/2$ is the local nozzle half-width along the horizontal centerline. This parameter was evaluated at a location one maximum nacelle radius upstream of the nozzle exit, where the difference in corner sharpness is largest. The incremental drag change with corner sharpness for the N_{QC} and modified N_{QC} nozzles was quite similar.

As mentioned previously, the unmodified N_{QC} nozzles were not exact scale representations of the QCSEE flight nozzles but had additional boattail projected area present. The combination of geometrical changes inherent in the modified N_{QC} nozzles resulted in reduced boattail projected area above the wing. Relative values of this area and the associated drag levels are indicated in figure 14. It is not possible to isolate the effects of boattail area from the other geometric changes between the N_{QC} and modified N_{QC} nozzles, so figure 14 only indicates general trends. It is reasonable to assume that the drag penalty associated with the correct boattail area would lie somewhere between the full-scale mark and the N_{QC} point, depending on the relative effect of boattail area compared to the effects of changes in sidewall boattail angle and flow kickdown angle. The proximity of the modified N_{QC} points to the geometrically

correct boattail areas is of interest. This proximity suggests that the QCSEE nozzles with external sidewall boattailing reduced to 2° might obtain a cruise drag penalty somewhere near these levels if the effects of kickdown angle are not important. This would amount to drag penalties between 12 and 14 percent of net thrust for the RC1 nozzle and between 6 and 8 percent for the baseline nozzle.

CONCLUDING REMARKS

In summary, it was found that USB nacelles with moderate nozzle boattail angles could be installed on a high-wing short-haul aircraft configuration with only a small cruise drag penalty. This type of nozzle would not have good low-speed powered-lift performance without the development of a flow deflector and exit area variation system. A high boattail angle nozzle representing the QCSEE RC1 configuration, which was designed for good powered-lift performance without a flow deflector, displayed large cruise drag penalties associated with boattail flow separation and regions of accelerated supercritical flow on the wing upper surface. A similar nozzle with rounder corners and reduced powered-lift performance, representing the QCSEE baseline nozzle, had significantly lower cruise drag. Additional test configurations indicated the possibility of improving cruise drag levels of the QCSEE-type nozzles by reducing the sidewall boattail angles and the boattail projected area above the wing.

REFERENCES

1. Wimpress, J. K.: Upper Surface Blowing Technology as Applied to the YC-14 Airplane. SAE Paper 730916, Oct. 1973.

2. Johnson, J. L., Jr.; and Phelps, A. E., III: Low-Speed Aerodynamics of the Upper-Surface Blown Jet Flap. SAE Paper 740470, Apr. 1974.

3. Skavdahl, H.; Wang, T.; and Hirt, W. J.: Nozzle Development for the Upper Surface Blown Jet Flap on the YC-14 Airplane. SAE Paper 740469, Apr. 1974.

4. Ciepluch, Carl C.: QCSEE Program. Aeronautical Propulsion. NASA SP-381, 1975, pp. 65-80.

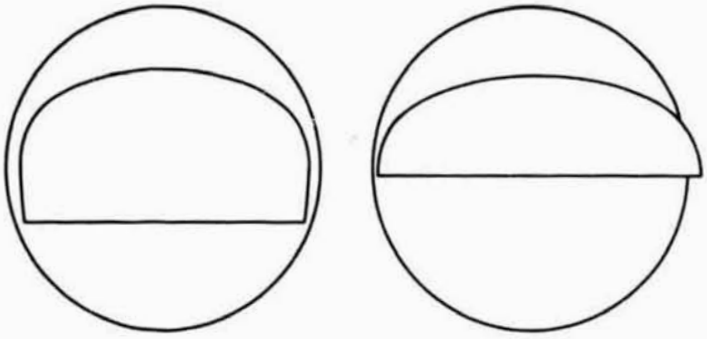

LOW-PRESSURE RATIO (QCSEE)	HIGH-PRESSURE RATIO (YC-14)
FAN P.R. = 1.37	FAN P.R. = 1.65
BYPASS RATIO = 10	BYPASS RATIO = 4
$\frac{A_{EXIT}}{A_{NAC}} = 0.5$	$\frac{A_{EXIT}}{A_{NAC}} = 0.3$
NOZZLE $AR_{EXIT} = 1.9$	NOZZLE $AR_{EXIT} = 3.2$

Figure 1.- Comparison of USB cruise nozzles.

Figure 2.- Wind-tunnel model.

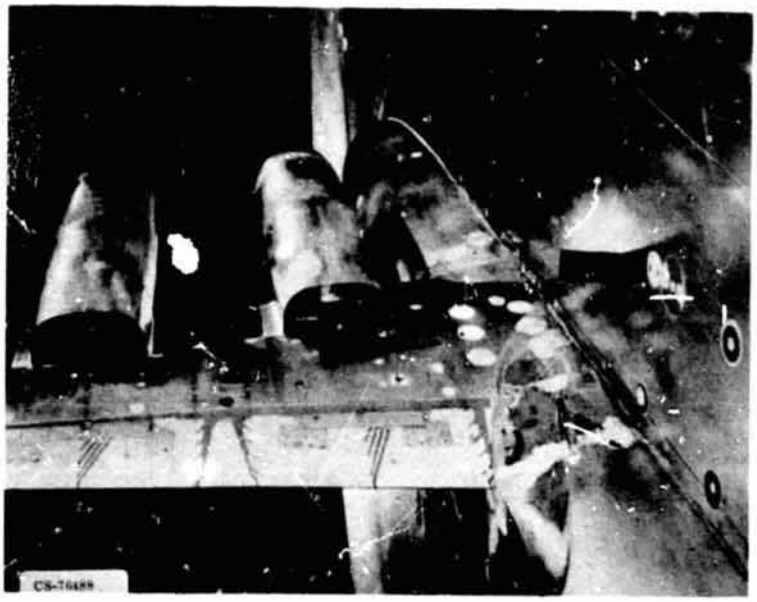

Figure 3.- Nozzle installation.

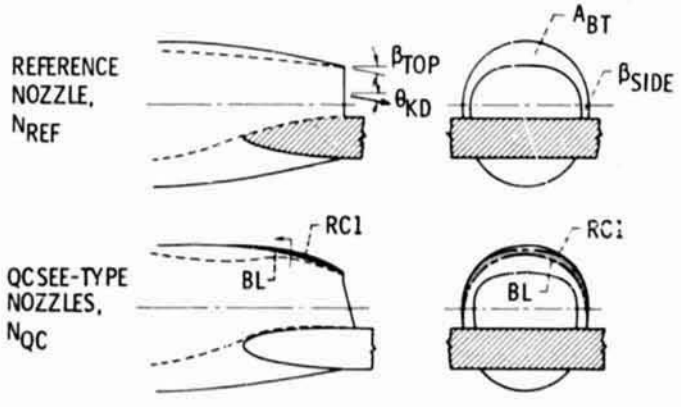

	β_{TOP}	β_{SIDE}	θ_{KD}	(A_{BT}/A_{NAC})
N_{REF}	11^0	2^0	3^0	0.214
$(N_{QC})_{BL}$	28^0	17^0	12^0	.282
$(N_{QC})_{RC1}$	28^0	17^0	12^0	.300

Figure 4.- Test nozzle configurations.

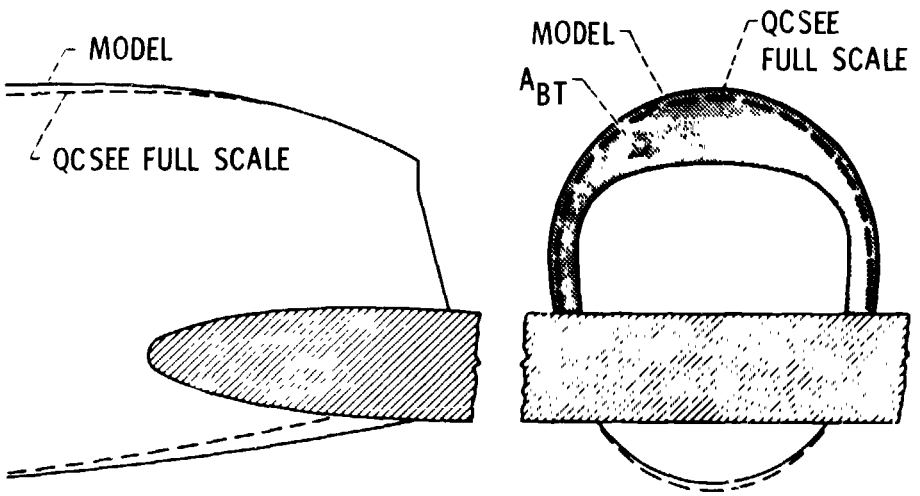

	$(A_{BT}/A_{NAC})_{MODEL}$	$(A_{BT}/A_{NAC})_{FULL\ SCALE}$
$(N_{QC})_{BL}$	0.282	0.237
$(N_{QC})_{RC1}$	.300	.252

Figure 5.- Comparison of model and QCSEE engine.

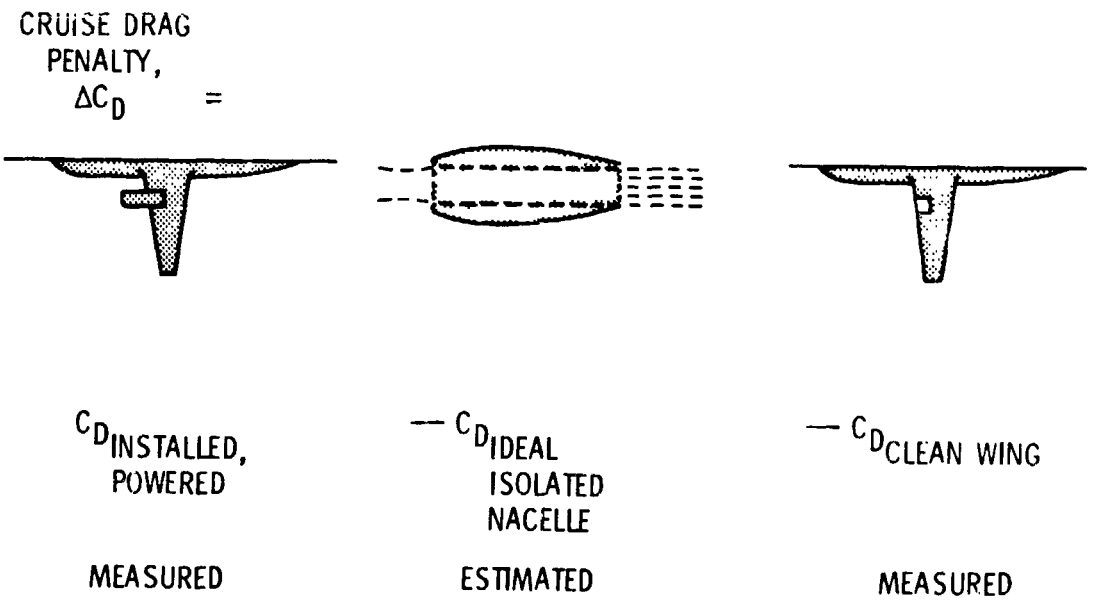

Figure 6.- Drag definition.

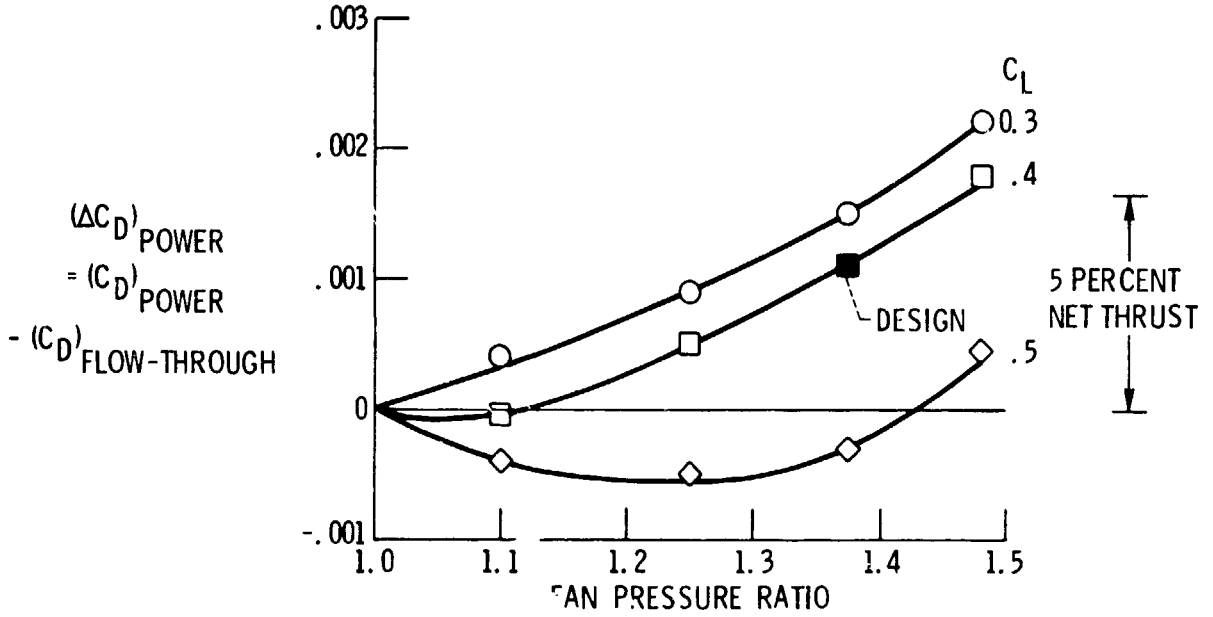

Figure 7.- Power effect; $(N_{QC})_{RC1}$ nozzles; 4-engine configuration; $M_0 = 0.7$.

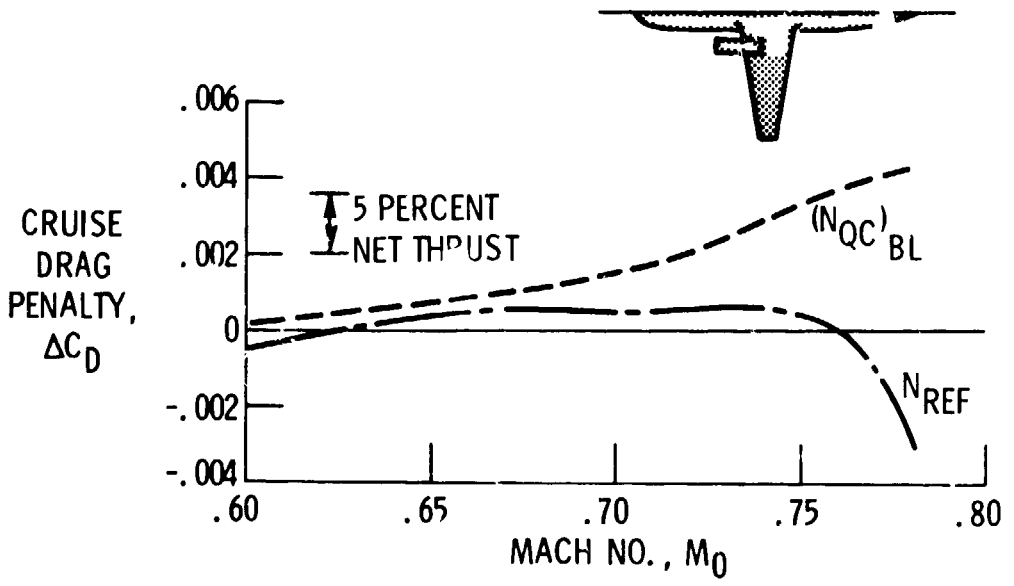

Figure 8.- Two-engine drag; FPR = 1.37; $C_L = 0.4$.

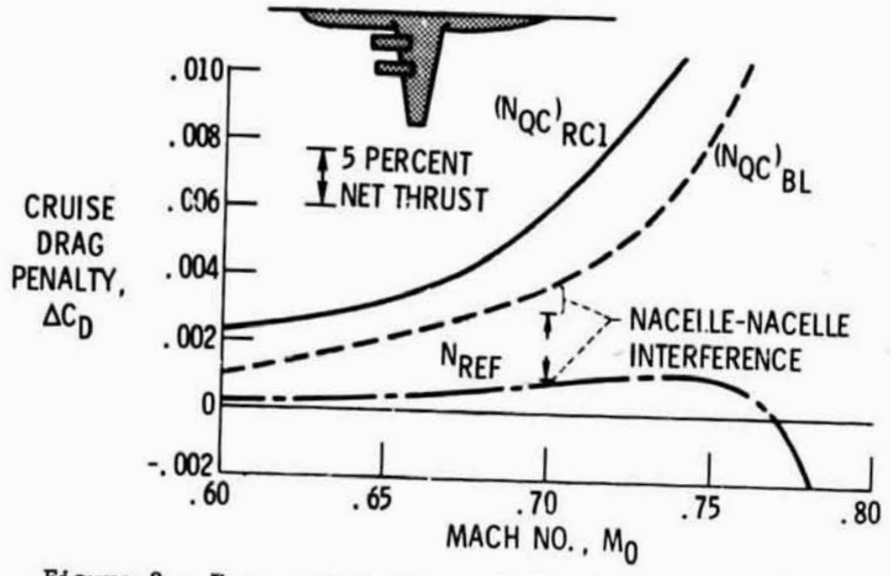

Figure 9.- Four-engine drag; FPR = 1.37; C_L = 0.4.

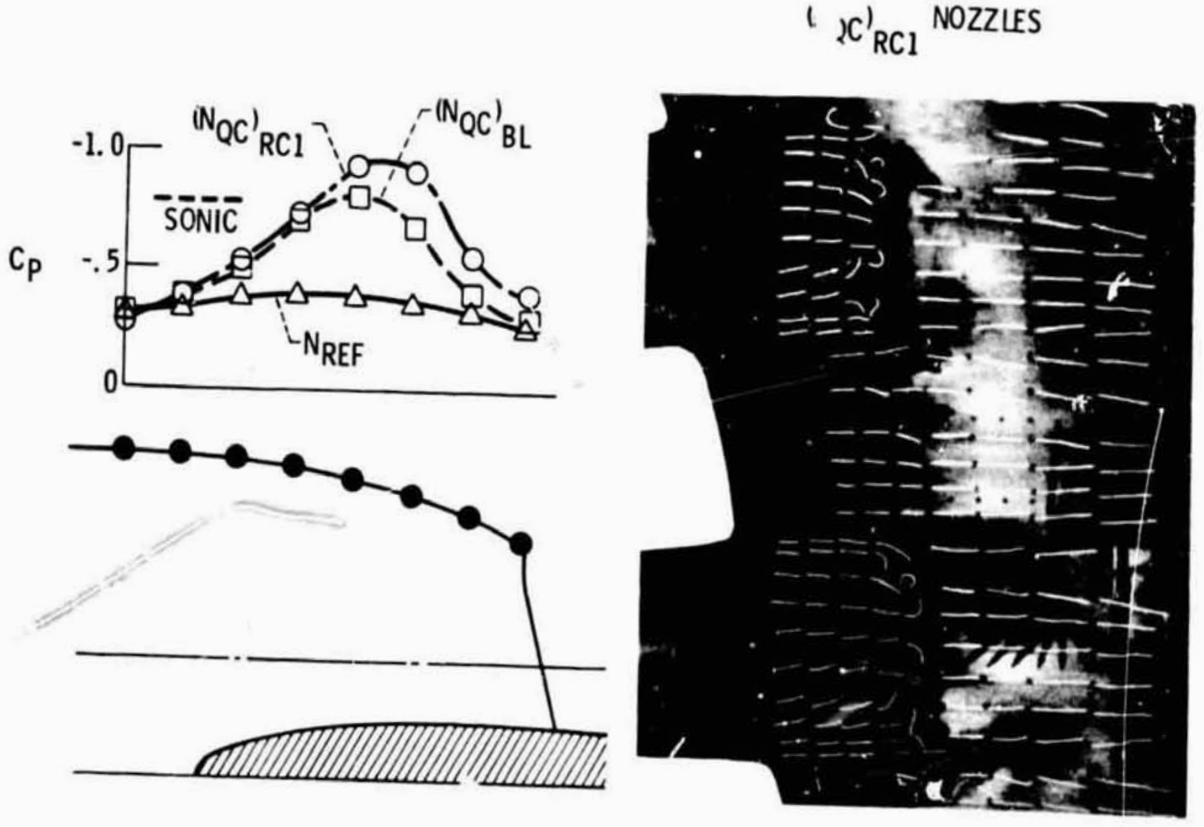

Figure 10.- Boattail separation; M_0 = 0.7; C_L = 0.4; FPR = 1.37.

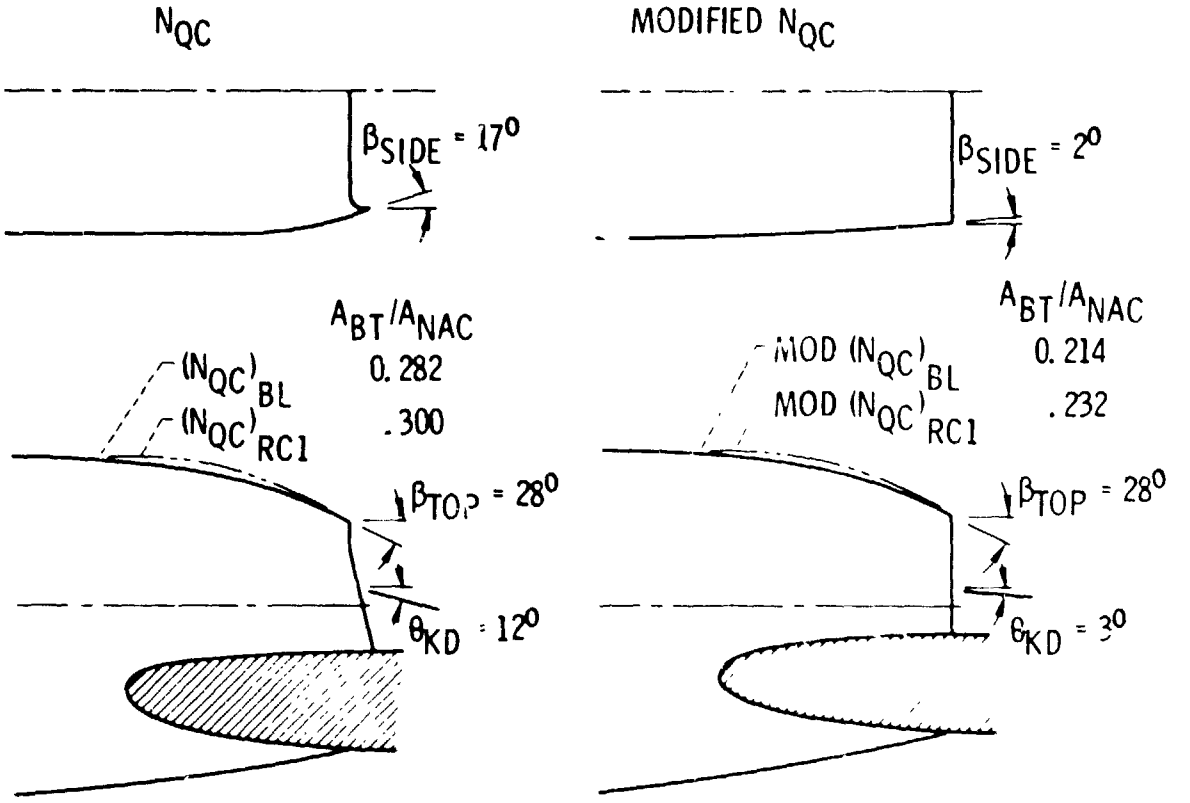

Figure 11.- Modified N_{QC} nozzles.

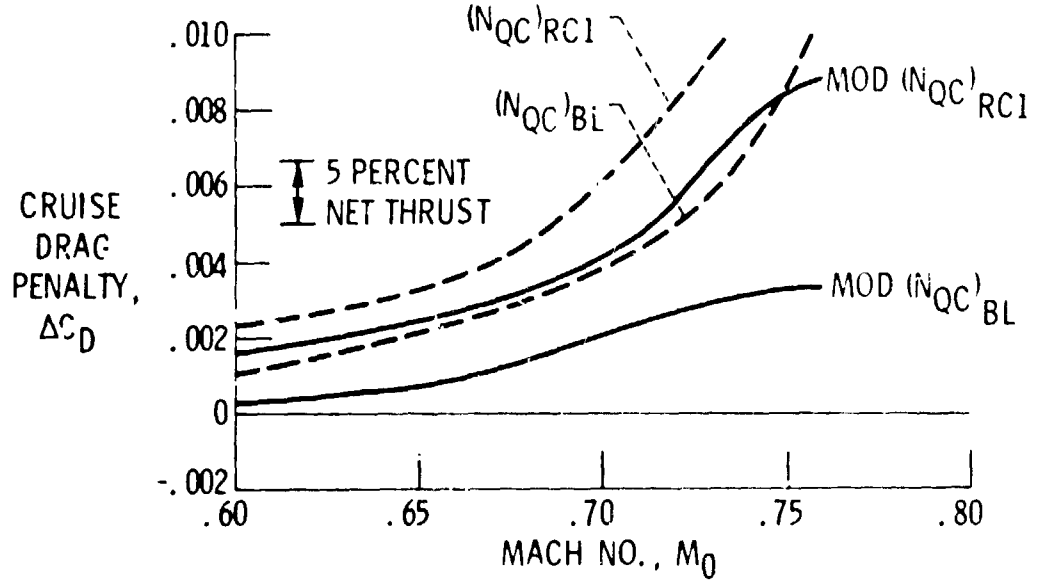

Figure 12.- Effect of N_{QC} nozzle modifications; 4-engine configuration; FPR = 1.37; $C_L = 0.4$.

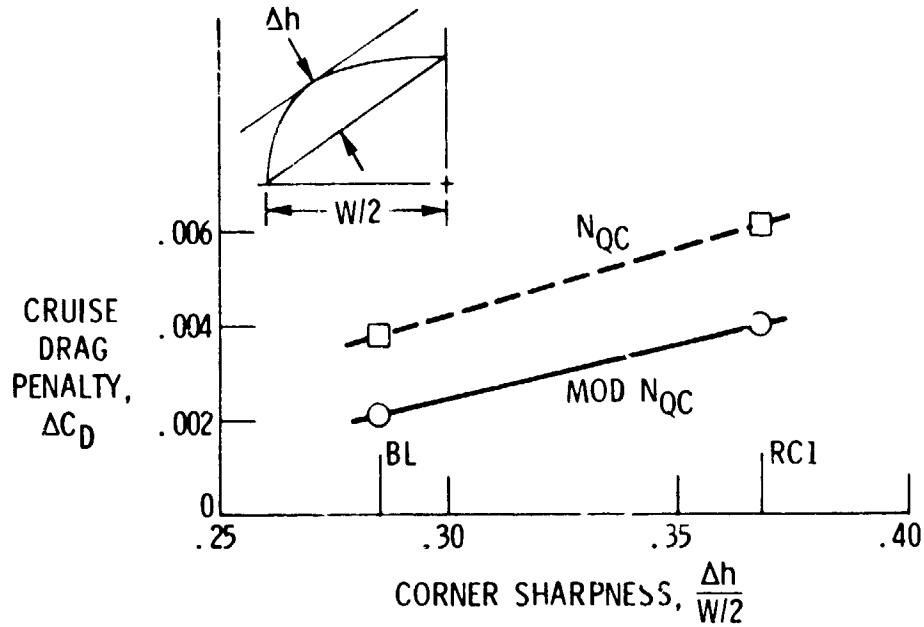

Figure 13.- Effect of corner sharpness; $M_0 = 0.7$; $C_L = 0.4$; FPR = 1.37.

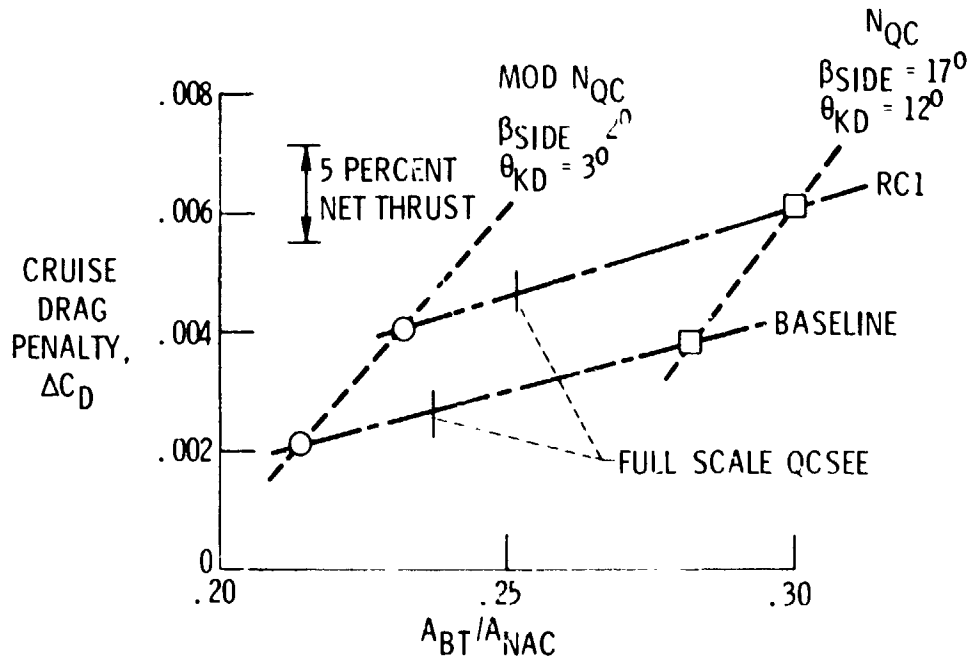

Figure 14.- Nozzle geometry effects; $M_0 = 0.7$; $C_L = 0.4$; FPR = 1.37.